DENTAL MATERIALS 35 (2019) 928–936

Available online at www.sciencedirect.com

ScienceDirect

journal homepage: www.intl.elsevierhealth.com/journals/dema

Modification of filler surface treatment of composite resins using alternative silanes and functional nanogels

Bruna Marin Fronza[a], Steven Lewis[b], Parag K. Shah[c], Matthew D. Barros[b], Marcelo Giannini[a], Jeffrey W. Stansbury[b,c,*]

[a] Restorative Dentistry Department, Piracicaba Dental School, University of Campinas, Piracicaba, SP, Brazil
[b] Craniofacial Biology Department, University of Colorado, Aurora, CO, United States
[c] Chemical and Biological Engineering, University of Colorado, Boulder, CO, United States

ARTICLE INFO

Article history:
Received 4 February 2019
Received in revised form
16 March 2019
Accepted 18 March 2019

Keywords:
Composite resin
Fillers
Methacrylates
Isocyanates
Nanogels
Surface treatment
Silanization
Polymerization
Stress
Mechanical properties

ABSTRACT

Objectives. This study probes how modifiedapproaches for filler surface treatment in dental composites based on alternative silanes and functional nanogel additives affects physicochemical properties of these materials with a focus on polymerization stress development.
Methods. Nanogels were synthesized from isobornyl methacrylate, ethoxylated bisphenol-A dimethacrylate and isocyanatoethyl methacrylate followed by partial further reaction with 2-hydroxyethyl methacrylate to provide both isocyanate and methacrylate functionalization. A barium glass filler (1̃ μm particle size) was treated with either γ-methacryloxypropyltrimethoxysilane (MPS), *N*-methylaminopropyltrimethoxy (MAP) or *N*-allylaminopropyltrimethoxy (AAP) silanes. The reactive nanogels were then covalently attached to the aminosilane-treated fillers. Surface treatment was characterized by thermogravimetric analysis (TGA) and diffuse reflectance infrared spectroscopy (DR-IR). Composites were formulated with 60 wt% of the various functionalized fillers and the materials were evaluated for polymerization kinetics, polymerization stress (PS), volumetric shrinkage, mechanical properties and photorheology. Data were evaluated by one-way ANOVA and Tukey's test at 5% significance level.
Results. Filler surface treatments were confirmed by TGA and DR-IR analyses. Nanogel-functionalized fillers significantly reduced PS up to 20%, while the degree of conversion and elastic modulus were not compromised. Similar storage modulus development during polymerization was observed among materials by photorheology although the rate of polymerization was significantly increased for nanogel-based treatments. A significant decrease

---

Abbreviations: PS, polymerization stress; MPS, γ-methacryloxypropyltrimethoxysilane; IBMA, isobornyl methacrylate; BisEMA, ethoxylated bisphenol-A dimethacrylate; IEM, isocyanatoethyl methacrylate; MAP, *N*-methylaminopropyltrimethoxysilane; AAP, *N*-allylaminopropyltrimethoxysilane; Tg, glass transition temperature; TGA, thermogravimetric analysis; BisGMA, bisphenylglycidyl dimethacrylate; TEGDMA, triethylene glycol dimethacrylate; DC, degree of conversion.

* *Corresponding author at*: University of Colorado School of Dental Medicine, Anschutz Medical Campus, 12800 E. 19th Ave./MS 8310, Aurora, CO 80045, USA.

E-mail addresses: bruna.fronza@hotmail.com (B.M. Fronza), lewistev@ohsu.edu (S. Lewis), parag.shah@colorado.edu (P.K. Shah), matthew.barros@ucdenver.edu (M.D. Barros), giannini@unicamp.br (M. Giannini), jeffrey.stansbury@ucdenver.edu (J.W. Stansbury).

https://doi.org/10.1016/j.dental.2019.03.007

in flexural strength was observed for amino functional silane groups; however, there was no statistical difference in strength for the MPS control group compared with the nanogel-modified composites.

Significance. Filler surface treatment modified with a reactive nanogel enables significant PS reduction, without compromise to degree of conversion or mechanical properties of dental composites.

1. Introduction

Composite resins have been used in dentistry as restorative materials for 50 years, with significant improvements over time. Initially, the majority of advances were focused on the filler systems to improve composite mechanical properties and longevity [1,2]. More recently, the focus has turned to the resin matrix with particular attention to reduce polymerization shrinkage and stress, and to improve materials' resistance to degradation in the oral environment [3]. The polymerization stress (PS) induces early gap formation at the resin-tooth bonded interface, which can cause post-operative sensitivity, facilitate staining and bacterial infiltration with the potential consequence of reduced clinical longevity [4–7]. Furthermore, PS can cause cusp deflection and cracks on the tooth structure and the material, which along with degradation may lead to fracture of the restoration or tooth [8,9].

Among the research strategies devoted to overcome these issues and improve resin composites performance, very few studies have focused on the coupling between the organic resin and inorganic fillers. In composite materials, fillers are commonly surface treated with γ-methacryloxypropyltrimethoxysilane (MPS) to provide a covalent linkage between both distinct phases. This link is fundamental to mechanical reinforcement and wear resistance, to slow the degradation process, and to promote stress transition from the more flexible organic matrix to the very stiff inorganic fillers [10–12]. However, the surface-bound methacrylate functional groups from MPS are relatively immobile, which places conformational restrictions on the resin matrix during polymerization resulting in a build-up of internal stresses. Likewise, this interface accumulates stress by itself as the fillers present the lowest compliance in a composite system [13].

A previous study demonstrated the application of flexible hyperbranched oligomers on the filler surface as an alternative coupling agent to lower PS of composites when incorporated with an experimental thiol–yne–methacrylate resin matrix [14]. Likewise, the use of a thiourethane-modified silane was also beneficial to reduce the PS of composites via a chain transfer mechanism [15]. Based on this concept of using the resin-filler interface not only as a linkage, but also as a source of compliance to minimize stress development during polymerization, here we contemplate the use of amine functional silanes associated with isocyanate-methacrylate nanogels as a filler surface treatment. The use of nanogels tethered to the functional silane surface on a filler provides a physical extension of the reactive methacrylate groups away from the surface to interact with the resin matrix. It also provides a hybrid nanogel-resin interphase due to facile monomer infiltration of and copolymerization with the nanogels localized on filler surfaces. Moreover, nanogels feature potential for PS reduction when used as additives in the resin [16,17].

Therefore, the objectives of this study were to modify the filler surface treatment using alternative silanes and reactive nanogel additives as a means to alter the physicochemical properties of composites loaded with the experimentally treated fillers. The hypotheses tested were as follows: (1) nanogel-functionalized fillers will reduce the PS of composites and (2) there will be no adverse effect on mechanical properties of composites with nanogel-functionalized fillers in comparison to analog composites with conventional methacrylate silane filler treatment.

2. Materials and methods

2.1. *Nanogel syntheses*

Nanogels were synthesized by a batch process from isobornyl methacrylate (IBMA; TCI America, Portland, OR, USA), ethoxylated bisphenol-A dimethacrylate (BisEMA; Esstech, Essington, PA, USA), and isocyanatoethyl methacrylate (IEM; TCI America) at 50:30:20 mol ratio. Azobisisobutyronitrile (AIBN; Sigma-Aldrich, St. Louis, MO, USA) at 1 mol% was used as thermal initiator. Free-radical polymerization was carried out in solution using 15-fold excess of methyl ethyl ketone solvent (MEK; Fisher Scientific, Waltham, MA, USA) at 80 °C and a stirring rate of 200 rpm. Methacrylate conversion during synthesis was followed (based on C=C peak area at 1637 cm^{-1}) in mid-IR spectra (Nicolet 6700, Thermo Scientific, Waltham, MA, USA) until 60% conversion was achieved. Nanogels were precipitated from the clear reaction mixture by dropwise addition into hexanes (15-fold excess; Fisher Scientific). Resulting precipitates were re-suspended in dichloromethane (BDH Chemicals, VWR Analytical, Radnor, PA, USA). In order to obtain reactive nanogels capable of copolymerization with methacrylate resins, 2-hydroxyethyl methacrylate (HEMA; TCI America) was added to the solution to partially convert the pendant isocyanate groups to urethane methacrylates. This reaction was conducted at room temperature for 12 h with a trace amount of dibutyltin dilaurate (Sigma-Aldrich) as catalyst. The polymer precipitation method was repeated, and residual solvent was removed completely under vacuum until the nanogels were obtained as dry powders. This step-wise nanogel construction and subse-

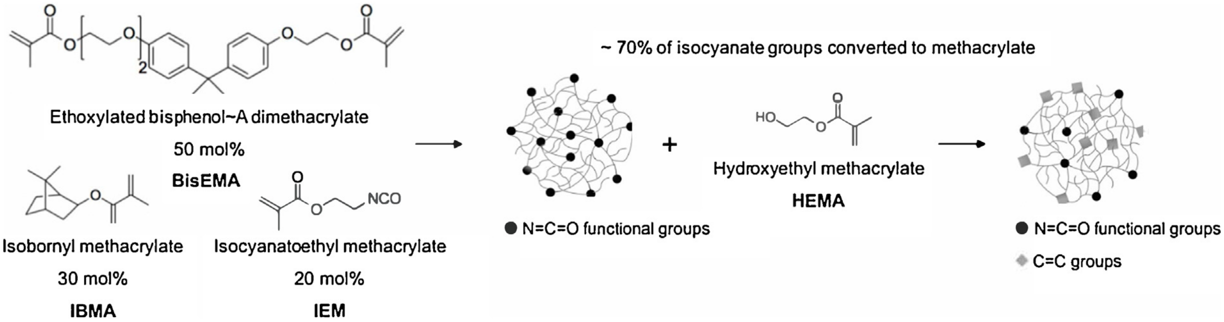

Fig. 1 – Structures of monomers used in the nanogel synthesis. At the first step internally crosslinked nanogels with chain-end isocyanate functionality is formed. This allows a route for reintroduction of functional methacrylate groups via the hydroxyl group from HEMA. The final nanogels obtained contain both isocyanate and methacrylate functionalities.

quent functionalization yielded nanogels appended with both isocyanate and methacrylate groups (Fig. 1).

The nanogels were characterized by single analysis using triple detector (refractive index, viscosity, light scattering) gel permeation chromatography (GPC; Viscotek, Malvern Instruments, Malvern, UK) in tetrahydrofuran (MilliporeSigma, Burlington, MA, USA) using a series of four columns spanning molecular weights of 10^4–10^7 with absolute Mw based on right/low angle light scattering detection calibrated with a 65 kg/mol poly(methyl methacrylate) standard.

Glass transition temperature (Tg) of nanogel ($n = 2$) was determined by dynamic mechanical analyzer (DMA; Perkin Elmer 8000, Perkin Elmer, Waltham, MA, USA) by sandwiching 10 mg of the bulk nanogel powders in a thin metallic pocket that was then subjected to single cantilever cyclic displacement of 50 μm at 1 Hz. The nanogel was heated from 0 to 150 °C with tan δ data collected in the second cycle of heating at 2 °C/min in air.

2.2. Filler surface treatment

A bare barium glass filler (1 μm, Lot. 161130, Dentsply Sirona, York, PA, USA) was treated with three different silanes (Fig. 2): the conventional γ-methacryloxypropyltrimethoxysilane (MPS; Sigma-Aldrich) as a conventional methacrylate functionalized silane coupling agent, as well as two aminosilanes; *N*-methylaminopropyltrimethoxysilane (MAP; Gelest, Morrisville, PA, USA) and *N*-allylaminopropyltrimethoxysilane (AAP; Gelest), which also contains a pendant vinyl group. Fillers were treated with 5 wt% silane (relative to filler) in cyclohexane (Sigma-Aldrich) using *N*-propylamine (Sigma-Aldrich) at 2 wt% as catalyst. The mixture was stirred at room temperature for 30 min and then at 60 ± 5 °C for additional 30 min at atmospheric pressure and then placed in a rotary evaporator at 60 °C to remove the solvent and volatile by-products. The fillers were washed with acetone (Sigma-Aldrich) multiple times to remove any physically adsorbed silane. The powder was then heated at 95 ± 5 °C for 1 h, and finally dried at 80 °C in a vacuum oven for 23 h.

Pendant methacrylate (MPS) or amine (MAP and AAP) groups at filler surface were reacted with nanogels. The secondary amino functional silanes (MAP and AAP) covalently connect with the isocyanate-functionalized nanogels forming substituted urea linkages. The reaction was confirmed by proton nuclear magnetic resonance spectroscopy (^{1}H NMR; detailed methodology described in the Appendix in Supplementary material). For the MPS control filler, the same surface treatment protocol was used with covalent attachment of the nanogels likely reliant on isocyanate reaction with surface-bound silanol groups associated with the MPS coverage. The application of the functional nanogel to the various silane-treated fillers was carried out using a filler to nanogel weight ratio of 1:3 in toluene at room temperature for 4 h with a trace amount of dibutyltin dilaurate. Once again, multi-step acetone washing of the treated fillers was performed to remove any unbound nanogel, which was then followed by solvent removal during 24 h storage under vacuum.

Filler surface treatments were identified by diffuse reflectance Fourier transform infrared spectroscopy (DR-IR; Nicolet 6700) spectroscopy. Spectroscopic grade KBr (Sigma-Aldrich) and fillers were ground together and placed in the DR-IR accessory. Single analysis spectra were taken at 8 cm^{-1} resolution, 64 scans, over the range of 4000–1350 cm^{-1}, using KBr as background. Thermogravimetric analysis (TGA; Pyris 7 TGA, Perkin Elmer) was used to determine the amount of silane and/or nanogel on surface of treated fillers. Samples (5 ± 1 mg) were placed in platinum pans in nitrogen atmosphere flow of 20 ml/min and heated from 50 °C to 850 °C with a heating rate of 10 °C min^{-1}. The mass loss, which corresponds to loss of the organic surface coating, as a function of temperature was recorded and normalized to the mass loss profile of the untreated filler.

2.3. Resin and composite formulations

A resin blend with bisphenylglycidyl dimethacrylate (BisGMA; Sigma-Aldrich) and triethylene glycol dimethacrylate (TEGDMA; Sigma-Aldrich) at 70:30 mol ratio was formulated. The photoinitiator system consisted of camphorquinone (0.3 wt%; Sigma-Aldrich) and ethyl 4-dimethylaminobenzoate (0.8 wt%; Sigma-Aldrich). Composites were prepared at 60 wt% loading of either the silane-only treated fillers or the analogous nanogel-functionalized fillers, which were incorporated to the resins with the aid of a mechanical mixer (DAC 150 Speed Mixer, Flacktek, Landrum, SC, USA) for 5 min at 2000 rpm.

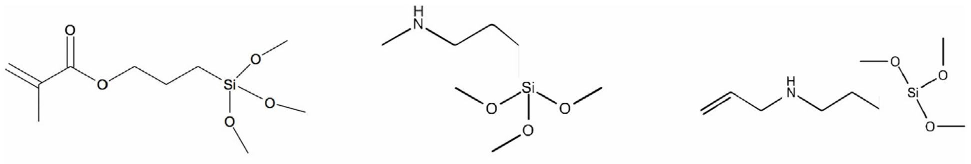

γ-methacryloxypropyltrimethoxy η-methylaminopropyltrimethoxy η-allylaminopropyltrimethoxy

MPS **MAP** **AAP**

Fig. 2 – Chemical structures of the silane agents.

2.4. *Resin and composite testing*

Polymerization kinetics was monitored in by Fourier transform near-infrared spectroscopy (FT-NIR, Nicolet 6700) in specimens (n = 3) of 6 mm in diameter and 0.8 mm thick laminated between two glass slides. The area of the methacrylate vinyl absorbance peak centered at 6165 cm^{-1} [18] was used to follow the real-time polymerization reaction continuously for 10 min. Specimens were photo-activated for 20 s at an incident irradiance of 1470 mW/cm^2 at 430–480 nm wavelength (Elipar DeepCure-S LED, 3M ESPE, St. Paul, MN, USA). Measurements were taken at a wavenumber resolution of 4 cm^{-1} with 32 scans per spectrum acquired for static scans before and after polymerization to measure degree of conversion (DC) and 2 scans per spectrum for polymerization kinetics, which provides a data acquisition rate of 2 Hz. The polymerization rate maximum (R_{Pmax}) was calculated as the maximum in the first derivative of the conversion vs. time curve.

PS (n = 5) was evaluated with a tensometer (Volpe Research Center, American Dental Association Health Foundation, Chicago, IL, USA) using 6 mm diameter glass rods. Rods were sectioned into lengths of 28 and 5 mm, in which one surface of the 28-mm long rods was polished with a sequence of silicon carbide abrasive papers and felt disks in order to optimize the transmission through the rod end into the specimen during light-activation. The opposite surfaces of the 28- and 5-mm rods were polished with abrasive papers to create a rough surface, followed by silane application (Fusion, Taub Products, Jersey City, NJ, USA. The 28 mm rod were attached to the lower clamp of the tensometer and the 5 mm rods to the upper clamp. Each material was placed between the rods with a Centrix syringe at 1 mm thickness. The tip of the light-curing unit was positioned in contact with the polished lower rod. Force development was monitored for 10 min from the beginning of photo-activation (20 s), and the maximum nominal stress (MPa) was calculated by dividing the maximum force value recorded by the cross-sectional area of the rods.

Volumetric shrinkage (n = 5) was evaluated with a non-contact linear variable differential transducer-based linometer (Academic Center for Dentistry, Amsterdam, NL). Composites were placed onto an aluminum disc in the linometer and covered with a glass slide, which was adjusted to produce a specimen disc of approximately 1 mm thickness × 6 mm diameter. All specimens were light-activated for 20 s. The displacement caused by linear shrinkage during polymerization was measured and converted to the corresponding volumetric shrinkage. The dynamic shrinkage data was recorded during and extending beyond the irradiation interval for a total period of 10 min.

A rheometer (ARES, TA Instruments, New Castle, DE, USA) was used to assess the photorheology of the composites (n = 2). Materials were placed between two 20 mm parallel quartz disc plates and tested in shear at a frequency of 100 rad/s with 10% strain (ensuring a linear viscoelastic regime), while being photopolymerized at 5 mW/cm^2. An optical apparatus [19] allowed both curing light and FT-NIR direct transmission access to the specimen within the photorheometer, which provides degree of conversion concomitantly with storage modulus development.

Flexural strength and elastic modulus (n = 5) were determined by the three-point bending test. Bar specimens (n = 5) were fabricated (2 mm × 2 mm × 25 mm) between glass slides and polymerized with three overlapping 20 s light exposures each sides glass side, according to ISO 4049 [20]. Specimens were stored dry for 24 h in dark containers at room temperature. The three-point bending test was performed on a universal testing machine using a span of 20 mm and a crosshead speed of 1 mm/min (MTS Mini Bionix II, MTS, Eden Prairie, MN, USA). The flexural strength (FS) in MPa was then calculated as:

$$\mathrm{FS}\,(\sigma) = \frac{3F\iota}{2bh^2}$$

where F represents load at fracture (N), ι is the span length, and b and h are the width and thickness of the specimens, respectively.

The elastic modulus (E) in flexural was determined from the slope of the initial linear portion of stress–strain curve.

$$\mathrm{E} = \frac{F\iota^3}{4bh^3d}$$

where F is the load at some point on the linear region of the stress–strain curve, d the slack compensated deflection at load F, and ι, b, and h are as defined above.

2.5. *Statistical analysis*

Normal distribution was assessed by Shapiro–Wilk test and Brown–Forsythe's method was used to analyze the presence of equal variance. Data from degree of conversion, $R_{Pmax,}$ PS, volumetric shrinkage, elastic modulus, and flexural strength were evaluated using One-way ANOVA tests (factor: composite, 6 levels). Where appropriate, Tukey post-hoc tests were applied in order to detect pair-wise mean differences among the groups. For all statistical testing, a pre-set, global significance level of 5% was used.

3. Results

GPC analysis (Table 1) demonstrates that repeated production of the functional nanogels produced similar and relatively narrow distributions of very high-molecular-weight polymer with discrete particle size of approximately 17 ± 1 nm. The low Mark–Houwink exponent values indicates the highly branched, globular structures that are characteristic of these nanogel materials. DMA (Table 1) of nanogel powders revealed consistent Tg values of 57–63 °C.

The extent of filler surface treatment was estimated by TGA as 0.8–1.3 wt% for silanes, and 2.8–4.7 wt% for nanogel-functionalized fillers (Fig. 3A). The major weight loss associated with nanogel treatment starts around 250 °C, which further confirms that nanogels are reacted to the surface. DR-IR spectra (Fig. 3B) show free silanol groups (3742 cm^{-1}) for the untreated filler, which were effectively consumed after silanization. Methacrylate carbonyl peak at 1706 cm^{-1} (indicated by *) is present for MPS and all nanogel-functionalized fillers. Multiple aliphatic peaks (2856–2962 cm^{-1}) are observed for the MPS coated filler and these aliphatic peaks are clearly present at significantly higher concentrations following nanogel addition to the surface.

Properties results of composites are presented in Table 2. After 10 min polymerization kinetics evaluation (Fig. 4A), there was no statistically significant differences among groups for degree of conversion. Although, the rate of polymerization (Fig. 4B) was significantly higher for nanogel-functionalized fillers in comparison with its respective silane-only surface treatment. Nanogel-functionalized fillers were able to significantly reduce the PS, with the lowest values found for MPS and MAP associated with nanogels (Fig. 3C). However, the filler surface treatment did not affect the observed volumetric shrinkage (Table 2, Fig. 3D).

Regarding the mechanical properties, flexural strength of MPS silane and all treatments with nanogel additives provided significantly higher values, while the amino functional silane MAP presented the lowest. Nonetheless, the filler surface treatment did not affect the elastic modulus of the materials. Real-time photorheology during photocuring demonstrates similar modulus evolution along with degree of conversion and polymerization reaction progression for all experimental composites (Fig. 5A and B).

4. Discussion

The coupling agent between resin matrix and fillers represents the minor portion of the overall composite formulation; however, it serves an essential role in achieving the robust mechanical performance that is demanded of dental composite restoratives. Here, the modification of the resin-filler interface with amino-functional silanes allowed the controlled introduction of a single layer interphase since the nanogels offer no interparticle interactions. This nanogel-derived surface layer contributes negligible dimension to the overall filler particle size yet, this approach significantly reduced PS, without compromise to the mechanical properties of the composites. Therefore, the hypotheses of the study were accepted.

Nanogel functionalized fillers were able to significantly reduce the PS compared to the controls with silane treatment only (Table 2; Fig. 4C). The PS development and its magnitude are dependent on volumetric shrinkage along with evolution of elastic modulus, with both properties reliant on the degree of conversion [21,22]. Notably, there was no significant decrease in volumetric shrinkage or elastic modulus for the experimental materials (Fig. 4D; Table 2). Volumetric shrinkage is determined by the initial concentration of reactive groups in the composite overall as well as the degree of conversion reached during polymerization. Since the ratio of resin to the inorganic component of the filler do not differ substantially among the groups here, the starting reactive group density is comparable. This along with the similar levels of limiting conversion achieved across the series of composites studied here, means a reduction in shrinkage is not expected. Also related to this, the equivalence of the elastic modulus results for all the materials indicates that the polymer network density and quality is not affected by the presence of the nanogel-modified filler surfaces (Table 2; Fig. 5). It is worth noting that the Tg of the bulk nanogels offers a reasonably good match to the Tg obtained when the BisGMA/TEGDMA resin is photocured to its vitrification limiting conversion.

Because neither shrinkage nor modulus are altered for composites with the nanogel-modified filler, we consider that the introduction of a nanogel interphase provides a stress relaxation mechanism that operates during the course of photopolymerization (Fig. 4C). Nanogels are synthesized in a solution polymerization process, which results in a swellable structure. Once dispersed in resin, the nanogel polymeric particles, are swollen by monomer [23], which presumably occurs whether the nanogels are freely dispersed in the resin phase or tethered to the filler surface. This means an effective volume fraction of the monomer-swollen nanogel rather than a simple calculated volume fraction should be considered, which may have contributed to the reduction in stress. Additionally, the monomer swollen nanogels function as a transition phase between the resin and filler in terms of the local reaction rate as well as the evolving Tg and mechanical properties. These features along with the highly branched structure of the nanogels may allow compliant interfacial zone during polymerization that can internally absorb some of the developing stress. An important component of this is likely the physical displacement of the copolymerizable methacrylate groups in the nanogels away from the filler surface, which would enable a degree of compliant behavior.

Nanogels were synthesized from a mono-functional monomer (IBMA) and a di-functional crosslinker (BisEMA), with addition of IEM to introduce isocyanate functional groups (Fig. 1). In order to avoid macrogelation and control nanogels size, a 15-fold excess of MEK solvent was used along with a restriction of the reaction to 60% conversion. Chain transfer agents, such as alkyl thiols, are commonly used to help control nanogel molecular weight and size [17]; however, thiols would be consumed by the isocyanate groups from IEM and thus, the chain transfer agent was avoided here. Despite of use of the higher dilution in the nanogel synthesis as compared with

Table 1 – Gel permeation chromatographyparameters and glass transition temperature of nanogels.

	M_w (kg/mol)	PDI	Rh (nm)	MH-α	Tg (°C)
Batch 1	484.5	1.48	9.08	0.49	57.3
Batch 2	428.8	2.01	8.24	0.23	63.3
Batch 3	400.8	1.99	8.18	0.40	57.9
Batch 4	426.9	1.76	8.45	0.46	57.1
Average	435.2	1.81	8.49	0.40	58.9

Molecular weight (M_w), polydispersity index (PDI), hydrodynamic radius (Rh), Mark–Houwink exponent (MH-α), and glass transition temperature (Tg). GPC data represent single analyses of multiple nanogel batches while the Tg data reported for each batch represent averages of duplicate runs.

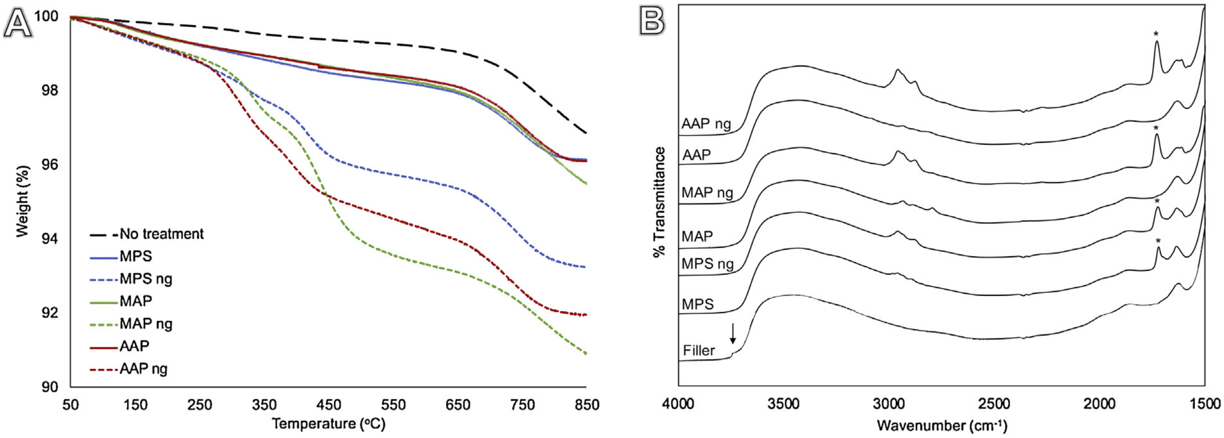

Fig. 3 – Thermogravimetric analysis displays weight loss of fillers as function of temperature increase. Filler surface treatment is estimated as 0.8–1.3 wt% for silanes and 2.8–4.7 wt% for nanogel additives (A). Diffuse reflectance spectroscopy spectra filler surface treatments. The non-treated fillers show the free silanol groups (3742 cm^{-1} peak indicated by arrow). The methacrylate carbonyl peak at 1706 cm^{-1} (indicated by *) is identified for MPS, MPS ng, MAP ng, and AAP ng. Multiple aliphatic peaks (2856–2962 cm^{-1}) can also be observed in higher intensity for nanogel treatments.

Table 2 – Mean (standard deviation) for degree of conversion (DC), maximum polymerization rate (R_{Pmax}), volumetric shrinkage (VS), polymerization stress (PS), flexural strength (FS) and elastic modulus (EM) of composites.

One-way ANOVA	DC (%) $p = 0.226$	R_{Pmax} (%/s) $p < 0.001$	VS (%) $p = 0.829$	PS (MPa) $p < 0.001$	FS (MPa) $p < 0.001$	EM (GPa) $p = 0.430$
MPS	65.5 (1.1)	11.0 (0.4) bc	4.1 (0.1)	2.3 (0.1) b	140.3 (18.3) a	6.0 (0.5)
MPS ng	64.1 (0.6)	13.1 (0.3) a	4.1 (0.1)	1.7 (0.1) d	132.5 (14.2) a	6.0 (0.8)
MAP	65.1 (0.5)	9.5 (0.3) d	4.1 (0.1)	2.6 (0.07) ab	82.8 (6.9) c	5.8 (0.8)
MAP ng	65.3 (0.3)	11.6 (0.5) bc	4.1 (0.2)	1.7 (0.1) d	127.2 (13.2) ab	6.2 (0.2)
AAP	65.2 (0.2)	10.7 (0.2) cd	4.0 (0.3)	2.5 (0.1) a	107.9 (2.4) b	6.7 (0.7)
AAP ng	64.0 (1.6)	12.4 (1.0) ab	4.1 (0.1)	2.0 (0.1) c	122.1 (10.6) ab	6.0 (0.8)

Within a column, means followed by the same letter are not statistically different ($p > 0.05$).

previous nanogel synthetic procedures, the molecular weights of the functional nanogels are approximately an order of magnitude greater than those that can be produced with a chain transfer agent under much more concentrated reaction conditions. The use of isocyanate nanogel functionality here was to produce substituted urea linkages through reaction with the secondary amine functional silanes on the filler surface, ultimately forming a polyurea-based interphase. Polyureas are widely used in materials science to produce soft elastomers, rigid thermosets, and foams [24]. Urea linkages have been found to be more hydrolytically stable than the ester bonds found in methacrylate structures, which are readily hydrolyzed in either basic or acidic solutions. The hydrolysis process diminishes material properties over time and ultimately leads to mechanical failure [25–27]. In this way, this alternative linkage has potential advantages for application at the critical filler-resin interface.

Notwithstanding, it is acknowledged that the pervasive use of methacrylate resins as the resin phase component of dental composites requires accommodation by coupling agent. Therefore, methacrylate groups were introduced into the nanogel structures via partial conversion of the pendant isocyanates through reaction with hydroxyl groups of HEMA. This provides the nanogels appropriate orthogonal functionality to covalently attach to the filler while presenting direct copolymerizabilty with the resin matrix to promote proper mechanical properties. However, even when these isocyanate/methacrylate functional nanogels were added to MPS

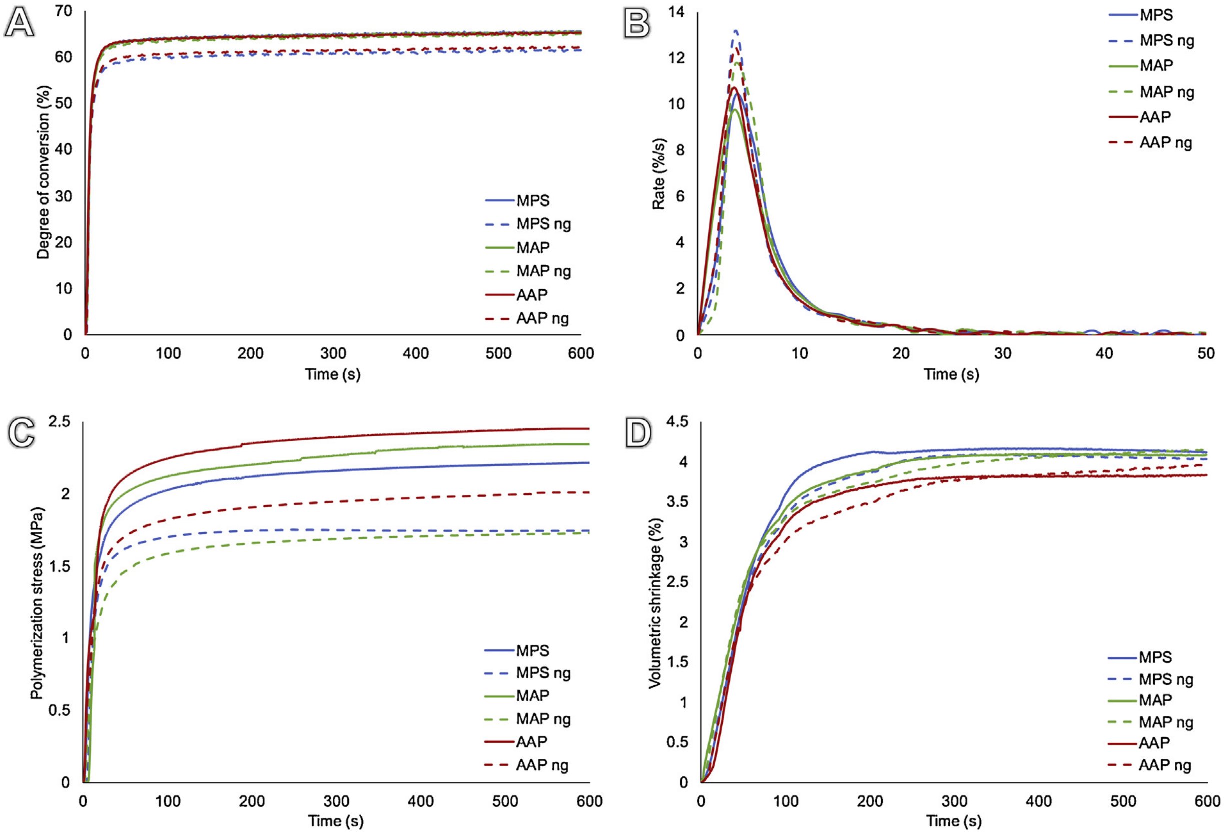

Fig. 4 – Degree of conversion (A) and rate of polymerization (B), polymerization stress development (C), and volumetric shrinkage (D) as function of reaction time for composites with different surface filler treatments. Notably, there is a reduction in polymerization stress for groups with nanogel-functionalized fillers.

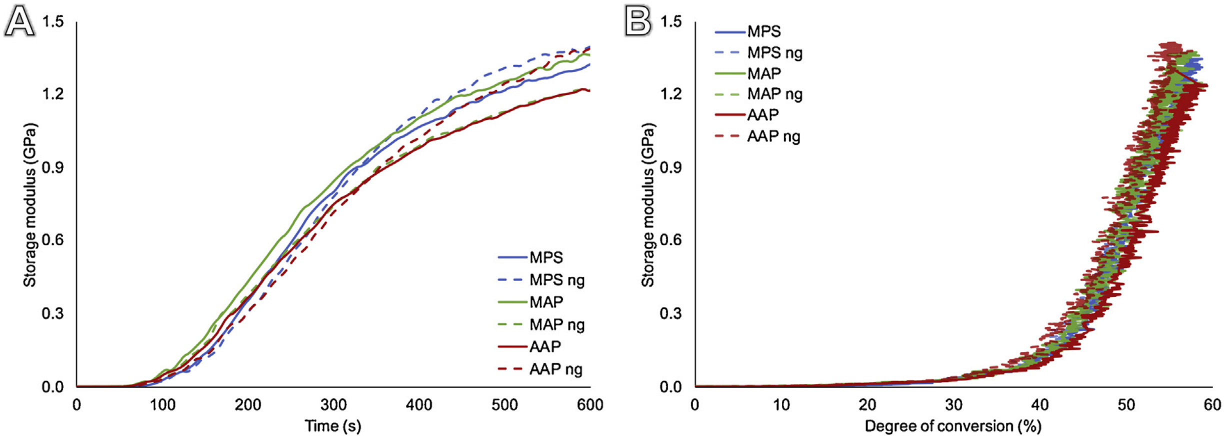

Fig. 5 – Photorheometric analysis demonstrates the storage modulus development as the reaction progresses (A), as well as storage modulus along with conversion acquirement (B). Note that the elastic modulus development and final values are similar to all materials, independent of filler surface treat.

silanated fillers, the mechanical properties obtained for the photocured composites indicate that suitable coupling was achieved between the filler and matrix phases (Table 2). For the filler surfaces treated with MPS or AAP that likely provide residual silane-based vinyl groups as well as to the methacrylate groups within the tethered nanogel layer, this offers an additional point of connection with the resin matrix to insure a strong connection between the composite phases. This is highlighted by the good mechanical properties observed with the MPS and AAP silane-only surface treatments (Table 2), albeit without the benefit of reduced PS that is attributed to the tethered nanogels. The restoration of mechanical properties when the non-copolymerizable MAP surface treatment is modified by appending the reactive nanogel layer provides a good demonstration of the filler-bound nanogel interaction with resin while the good mechanical strength of the AAP-only filler surface treatment indicates effective copolymerization between the silanebased allyl groups and the methacrylate resin.

Furthermore, the final degree of conversion attained was also unaffected by silane type or nanogel-functionalized fillers (Table 2; Fig. 4A). However, the presence of nanogels does provide a significant increase in the photopolymerization rate (Table 2; Fig. 4B). Previous studies have demonstrated that the use of nanogel additives dispersed in a monomer matrix can enhance, reduce or leave polymerization rates unaltered [16,17]. As compared with neat monomer, the internal monomer-swollen nanogel domain presents a localized higher viscosity environment, particularly with the highly branched nanogels used here. Therefore, when polymerization is initiated, depending on the amount of nanogel added, varying proportions of monomer will be in this more mobility-restricted state and the overall auto-acceleration behavior would also vary accordingly [16,28].

The viscoelastic behavior of the material characterized by its resistance to flow in the initial stages of the reaction, is also an important factor for stress development [21,22]. Despite the differences in polymerization rate, the rheology during polymerization was not affected, as demonstrated by storage modulus acquirement over time as well as in terms of degree of conversion (Fig. 5). The effect of low amounts of nanogels in resin viscosity is minimal as is typically observed for globular hyperbranched or dendritic polymeric additives [17]. Likewise, no obvious differences in handling characteristics were noticed here for the experimental and control composites. Moreover, the final storage modulus acquired corroborates with results from the three-point-bending test, in which no differences in final modulus were observed between groups (Table 2).

Herein we evaluated filler surface modification with 1 μm glass fillers only, while modern dental composites are multicomponent mixtures of fillers with a distributed range of sizes. Further studies should check the proposed surface treatment that include fumed silica or other nano-scale particles, which feature a greater surface area and offer features such as enhanced filler packing and wear resistance. As mentioned, approaches that provide surface-active nanogels of even smaller dimension (<10 nm) would also be of interest. The current combination of amino silanes with isocyanate nanogels may provide a more reliable stable interface between filler and resin matrix; however, longer-term studies regarding hydrolytic and mechanical stability of both the modified silane-based interfaces and the nanogel-based interphases need to be carried out.

5. Conclusion

Filler surface treatment modified with reactive nanogels enables the potential for a significant reduction in PS, without compromise to degree of conversion or physical/mechanical properties of photocurable dental composites. The production of this substantial stress reduction based on a relatively small nanogel content located exclusively at the filler surface, highlights the potential of this intentionally engineered resin-filler interphase region in heterogeneous composite materials.

Acknowledgements

We would like to acknowledge Dentsply Sirona for donation of the glass filler used in this study. This research was supported by National Institutes of Health (NIH/NIDCRR01DE022348) and São Paulo Research Foundation (2015/23104-1 and 2016/05035-5).

Appendix A. Supplementary data

Supplementary material related to this article can be found, in the online version, at doi:https://doi.org/10.1016/j.dental.2019.03.007.

REFERENCES

[1] Chen MH. Update on dental nanocomposites. J Dent Res 2010;89:549–60.

[2] Ferracane JL. Resin composite — state of the art. Dent Mater 2011;27:29–38.

[3] Fugolin APP, Pfeifer CS. New resins for dental composites. J Dent Res 2017;96:1085–91.

[4] Ferracane JL, Hilton TJ. Polymerization stress — is it clinically meaningful? Dent Mater 2016;32:1–10.

[5] Fronza BM, Rueggeberg FA, Braga RR, Mogilevych B, Soares LE, Martin AA, et al. Monomer conversion, microhardness, internal marginal adaptation, and shrinkage stress of bulk-fill resin composites. Dent Mater 2015;31:1542–51.

[6] Goncalves F, Boaro LC, Ferracane JL, Braga RR. A comparative evaluation of polymerization stress data obtained with four different mechanical testing systems. Dent Mater 2012;28:680–6.

[7] Opdam NJ, van de Sande FH, Bronkhorst E, Cenci MS, Bottenberg P, Pallesen U, et al. Longevity of posterior composite restorations: a systematic review and meta-analysis. J Dent Res 2014;93:943–9.

[8] Oliveira LRS, Braga SSL, Bicalho AA, Ribeiro MTH, Price RB, Soares CJ. Molar cusp deformation evaluated by micro-CT and enamel crack formation to compare incremental and bulk-filling techniques. J Dent 2018;74:71–8.

[9] Rosatto CM, Bicalho AA, Verissimo C, Braganca GF, Rodrigues MP, Tantbirojn D, et al. Mechanical properties, shrinkage stress, cuspal strain and fracture resistance of molars restored with bulk-fill composites and incremental filling technique. J Dent 2015;43:1519–28.

[10] Antonucci JM, Dickens SH, Fowler BO, Xu HH, McDonough WG. Chemistry of silanes: interfaces in dental polymers and composites. J Res Natl Inst Stand Technol 2005;110:541–58.

[11] Condon JR, Ferracane JL. In vitro wear of composite with varied cure, filler level, and filler treatment. J Dent Res 1997;76:1405–11.

[12] Sideridou ID, Karabela MM. Effect of the amount of 3-methacyloxypropyltrimethoxysilane coupling agent on physical properties of dental resin nanocomposites. Dent Mater 2009;25:1315–24.

[13] Condon JR, Ferracane JL. Reduced polymerization stress through non-bonded nanofiller particles. Biomaterials 2002;23:3807–15.

[14] Ye S, Azarnoush S, Smith IR, Cramer NB, Stansbury JW, Bowman CN. Using hyperbranched oligomer functionalized

glass fillers to reduce shrinkage stress. Dent Mater 2012;28:1004–11.
[15] Faria ESAL, Dos Santos A, Tang A, Girotto EM, Pfeifer CS. Effect of thiourethane filler surface functionalization on stress, conversion and mechanical properties of restorative dental composites. Dent Mater 2018;34:1351–8.
[16] Liu J, Howard GD, Lewis SH, Barros MD, Stansbury JW. A study of shrinkage stress reduction and mechanical properties of nanogel-modified resin systems. Eur Polym J 2012;48:1819–28.
[17] Moraes RR, Garcia JW, Barros MD, Lewis SH, Pfeifer CS, Liu J, et al. Control of polymerization shrinkage and stress in nanogel-modified monomer and composite materials. Dent Mater 2011;27:509–19.
[18] Stansbury JW, Dickens SH. Determination of double bond conversion in dental resins by near infrared spectroscopy. Dent Mater 2001;17:71–9.
[19] Pfeifer CS, Wilson ND, Shelton ZR, Stansbury JW. Delayed gelation through chain-transfer reactions: mechanism for stress reduction in methacrylate networks. Polymer (Guildf) 2011;52:3295–303.
[20] ISO 4049. Dentistry — polymer-based restorative materials. International Organization for Standardization; 2009. p. 1–36.
[21] Braga RR, Ballester RY, Ferracane JL. Factors involved in the development of polymerization shrinkage stress in resin-composites: a systematic review. Dent Mater 2005;21:962–70.
[22] Stansbury JW. Dimethacrylate network formation and polymer property evolution as determined by the selection of monomers and curing conditions. Dent Mater 2012;28:13–22.
[23] Liu J, Rad IY, Sun F, Stansbury JW. Photo-reactive nanogel as a means to tune properties during polymer network formation. Polym Chem 2014;5.
[24] Chattopadhyay DK, Raju KVSN. Structural engineering of polyurethane coatings for high performance applications. Prog Polym Sci 2007;32:352–418.
[25] Ferracane JL. Hygroscopic and hydrolytic effects in dental polymer networks. Dent Mater 2006;22:211–22.
[26] Pegoretti A, Fambri L, Penati A, Kolarik J. Hydrolytic resistance of model poly(ether urethane ureas) and poly(ester urethane ureas). J Appl Polym Sci 1998;70:577–86.
[27] Podgorski M, Becka E, Chatani S, Claudino M, Bowman CN. Ester-free thiol-X resins: new materials with enhanced mechanical behavior and solvent resistance. Polym Chem 2015;6:2234–40.
[28] Moraes RR, Garcia JW, Wilson ND, Lewis SH, Barros MD, Yang B, et al. Improved dental adhesive formulations based on reactive nanogel additives. J Dent Res 2012;91:179–84.